The optomechanical design of the Quad-camera Wavefront-sensing Six-channel Speckle Interferometer (QWSSI)

Clark, Catherine, van Belle, Gerard, Horch, Elliott, Trilling, David, Hartman, Zachary, et al.

Catherine A. Clark, Gerard T. van Belle, Elliott P. Horch, David E. Trilling, Zachary D. Hartman, Michael Collins, Kaspar von Braun, Jeff Gehring, "The optomechanical design of the Quad-camera Wavefront-sensing Six-channel Speckle Interferometer (QWSSI)," Proc. SPIE 11446, Optical and Infrared Interferometry and Imaging VII, 114462A (13 December 2020); doi: 10.1117/12.2563055

SPIE.

Event: SPIE Astronomical Telescopes + Instrumentation, 2020, Online Only

The optomechanical design of the Quad-camera Wavefront-sensing Six-channel Speckle Interferometer (QWSSI)

Catherine A. Clark[a,b], Gerard T. van Belle[b], Elliott P. Horch[c], David E. Trilling[a], Zachary D. Hartman[b,d], Michael Collins[b], Kaspar von Braun[b], and Jeff Gehring[b]

[a]Northern Arizona University, 527 South Beaver Street, Flagstaff, AZ 86011, USA
[b]Lowell Observatory, 1400 West Mars Hill Road, Flagstaff, AZ 86001, USA
[c]Southern Connecticut State University, 501 Crescent Street, New Haven, CT 06515, USA
[d]Georgia State University, 25 Park Place South, Atlanta, GA 30303, USA

ABSTRACT

The Quad-camera Wavefront-sensing Six-channel Speckle Interferometer (QWSSI) is a new speckle imaging instrument available on the 4.3-m Lowell Discovery Telescope (LDT). QWSSI is built to efficiently make use of collected photons and available detector area. The instrument images on a single Electron Multiplying CCD (EMCCD) at four wavelengths in the optical (577, 658, 808, and 880nm) with 40nm bandpasses. Longward of $1\mu m$, two imaging wavelengths in the NIR are collected at 1150 and 1570nm on two InGaAs cameras with 50nm bandpasses. All remaining non-imaging visible light is then sent into a wavefront EMCCD. All cameras are operated synchronously via concurrent triggering from a timing module. With the simultaneous wavefront sensing, QWSSI characterizes atmospheric aberrations in the wavefront for each speckle frame. This results in additional data that can be utilized during post-processing, enabling advanced techniques such as Multi-Frame Blind Deconvolution. The design philosophy was optimized for an inexpensive, rapid build; virtually all parts were commercial-off-the-shelf (COTS), and custom parts were fabricated or 3D printed on-site. QWSSI's unique build and capabilities represent a new frontier in civilian high-resolution speckle imaging.

Keywords: Speckle imaging, wavefront-sensing, instrument design, diffraction-limited imaging, stellar properties

1. INTRODUCTION

In recent years, measurements of stellar multiplicity have been a focus for both stellar astrophysicists and exoplanet scientists. Stars preferentially form in groups, whether these are multi-star systems or clusters containing up to several million stars. When these multi-star systems host planets, unknown companions can hinder the detection and characterization of exoplanets.

Speckle interferometry, or speckle imaging, has proven to be one of the most effective methods for measuring stellar multiplicity. On large telescopes, a point source is seen as a speckle pattern, due to seeing-induced phase fluctuations across the wavefront. Labeyrie (1) first demonstrated that one can obtain information about the high-resolution structure of a star by performing Fourier analysis on these speckle patterns, pioneering the field of speckle interferometry.

Though this approach has proven to be a powerful technique for generating high-resolution images over the past few decades, speckle interferometry faced a limitation when attempting speckle imaging with intensified-CCDs or other microchannel-plate-based devices used in the 1990's: the 'dead-time effect' occurred in the pixels, causing bright speckles to preferentially look fainter. By the late 1990's and early 2000's, some speckle work was being done with low-noise CCDs to avoid this problem, especially when good photometry was needed (e.g. Horch, Meyer, and van Altena 2004 (2)). However, EMCCDs were introduced in speckle imaging by Tokovinin and

Corresponding author: Catherine A. Clark
catclark@lowell.edu

Optical and Infrared Interferometry and Imaging VII, edited by Peter G. Tuthill, Antoine Mérand, Stephanie Sallum, Proc. of SPIE Vol. 11446, 114462A · © 2020 SPIE
CCC code: 0277-786X/20/$21 · doi: 10.1117/12.2563055

Cantarutti (2008) (3) and quickly became the detector of choice in the following years. In an EMCCD, the charge associated with each detected photoelectron is amplified before the charge is read out. If the charge is considerably higher than the read noise, then one can detect individual photons, similar to the intensified systems, but with no dead time. In addition, since amplification is performed after detection but prior to readout, read noise no longer dominates (4).

The Differential Speckle Survey Instrument (DSSI) was developed to collect many speckle images on a single low-noise, large-format CCD, and to take advantage of regular CCDs' high quantum efficiency (5). DSSI was then updated to utilize two Andor EMCCDs (6), which have lower read noise and higher readout rates than regular CCDs. This proved to be a powerful method for increasing the signal-to-noise ratio for astrometric measurements, deriving component colors, and measuring subdiffraction-limited separations. In fact, DSSI was so successful that next-generation copies have been built for telescopes around the world: the NN-EXPLORE Exoplanet and Stellar Speckle Interferometer at the 3.5-m WIYN Telescope, 'Alopeke at the 8.1-m Gemini North telescope, and Zorro at the 8.1-m Gemini South telescope (7; 8; 9).

However, all speckle cameras, including DSSI and its family of successors, remain limited by the need to use narrow bandpass filters in order to record high-contrast speckle patterns. While DSSI pioneered the simultaneous collection of speckle patterns in two colors, there is still much of the visible spectrum that remains unused with it and other speckle cameras in use today. Speckle cameras have often been made flexible enough to be used at a variety of different telescopes with different f/ratios and pixel scales, but an instrument that could be designed specifically for a given telescope and tailored to its optical properties and pointing capabilities could make maximum use of its detector active area for speckle imaging, especially given the larger EMCCD formats that are available today. Further recent developments, such as the technique of aperture partitioning (10) and the suggestion of Lőbb (2016) (11) of using a wavefront sensor in combination with a speckle camera, point to the possibility of making speckle imaging substantially more sensitive than in the past.

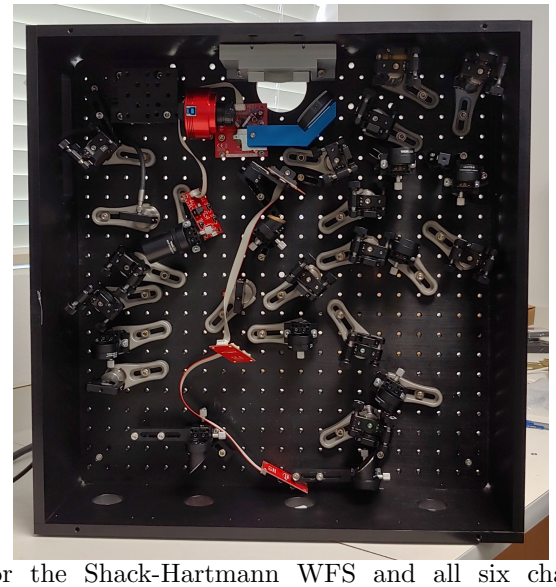

Figure 1: QWSSI's optics for the Shack-Hartmann WFS and all six channels are contained within a 22.84"×22"×6.5" optics box.

In an effort to make use of all light entering the instrument, and to capture recent developments to speckle imaging, we developed QWSSI. QWSSI represents a new frontier in speckle interferometry with four cameras, six filters (including two in the NIR), and simultaneous wavefront sensing, all contained within a compact 22.84"×22"×6.5" optics box (Figure 1). In Section 2, we describe the design philosophy and approach, optical design, electronics, and mechanical manufacturing. In Section 3, we characterize the setup of QWSSI, as well as the on-sky operations and data reduction. In Section 4, we present future work that will be carried out by QWSSI at the LDT.

2. DESIGN

2.1 Design Philosophy & Approach

Our design philosophy and approach was simple; we wanted to improve upon DSSI's design by making maximum use of photons entering the instrument. Furthermore, we wanted to add wavefront sensing for enhanced data reduction and improved reconstructed images. Finally, we wanted to implement these design ideas as inexpensively as possible.

In order to build QWSSI as economically as possible, we limited our design options to COTS components. These dramatically increase the speed, and lower the cost, of developing a new instrument. The total cost of the COTS optomechanical components and the notch filters was only $\sim \$16,480$. However, there are drawbacks to using COTS components; foremost among them is the fact that the visible-light Semrock filters are not imaging quality and degrade the speckle imager beam quality, limiting instrument sensitivity. Nevertheless, our intent on this particular design element has always been to initially use the rapidly available, Semrock COTS components for proof-of-concept operations of the overall system, and later purchase custom, imaging-quality filters to replace them.

We also utilized innovative manufacturing when needed, such as 3D printing, which is available to us through the Lowell Observatory machine shop. For design software, we used inexpensive shareware / freeware such as FreeCAD and Beam4. A breakdown of the costs to build QWSSI can be found in Table 1.

Table 1: Cost breakdown for QWSSI, minus detectors.

Part	Cost (USD)
Optomechanical parts	$ 13,100
Notch filters	$ 3,380
Computers	$ 1,500
Timing generator	$ 2,000
Baseplate	$ 500
Optics box	$ 5,000
Project box	$ 500
Total Cost	$ 25,980

A final element of our low-cost approach to QWSSI was to initially borrow its EMCCD detectors from DSSI, and leave the NIR channel unpopulated with detectors. However, we were successful in proposing for grant funding for both new EMCCDs, as well as NIR InGaAs detectors; these detectors represent a cost of roughly 9 times that of the other parts. It is worth noting that a visible-only system similar to QWSSI could be built for smaller telescopes with less expensive CMOS detectors for bright star binary research.

2.2 Optical Design

Inside the optics box, the f/6 beam from the telescope is collimated using an off-axis parabola. It is then split into its visible and NIR components using a VIS/NIR dichroic that reflects the NIR light. The NIR side of QWSSI essentially duplicates the current DSSI design, with two imaging wavelengths in the NIR split by a second dichroic, each passed through a narrow-band filter at 1150 and 1570nm, and then each NIR speckle image collected on separate FirstLight InGaAs cameras (C-RED 2s).

On the visible side of QWSSI, the collimated beam has four wavelengths at 577, 658, 808, and 880nm split off of it in succession, using filters with 40nm bandpasses. Each of these four channels are imaged onto separate quadrants of a single EMCCD. The remaining collimated light is then sent to the wavefront sensor (WFS), to be imaged on a second EMCCD (Figure 2). An achromatic design that makes use of off-axis parabolas is utilized for the beam to the WFS, which allows a wide bandpass to be used by the WFS. QWSSI utilizes Andor iXon Ultra 888 EMCCDs to image the visible channels and the WFS. Some design nuances are worth noting here:

- As noted in the previous section, the four narrowband filters are not imaging quality elements. Inspection of these filters with a Zygo shearing interferometer indicated that they deviate from a true optical flat by

1.2-2.2λ rms. However, this aberration is chiefly *spherical*, which when modeled out, a residual aberration of 0.03-0.06λ rms is indicated. As such, our remedy was to restrict our usage of these filters to a close to normal incidence as possible, which would allow for first-order correction of the spherical aberration through simple focus adjustment. Since our use wasn't completely at normal incidence, some coma and astigmatism does remain in the beam.

- Another deviation from the ideal normal incidence condition was with the four speckle beams relayed onto the imaging EMCCD. However, in this section of the optical design, the inherent nature of the speckle imaging system helps immensely: because of the magnification required to put a speckle image onto the imaging EMCCD, the focal length of the reimaging lens was very long. The resultant large f/number ($\sim$50) meant that the speckle image on the EMCCD had a very large depth of focus ($\sim$2mm)*, sufficient to tolerate a tilted incidence angle; at a 25mm offset from the centerline perpendicular to the EMCCD detector, the focus offset from one side of the image to the other side of the image in a given quadrant is a factor of ten less than this depth of focus.
- Since each imaging beam is narrowband, inexpensive stock achromat lenses were of sufficient quality for a diffraction limited beam.

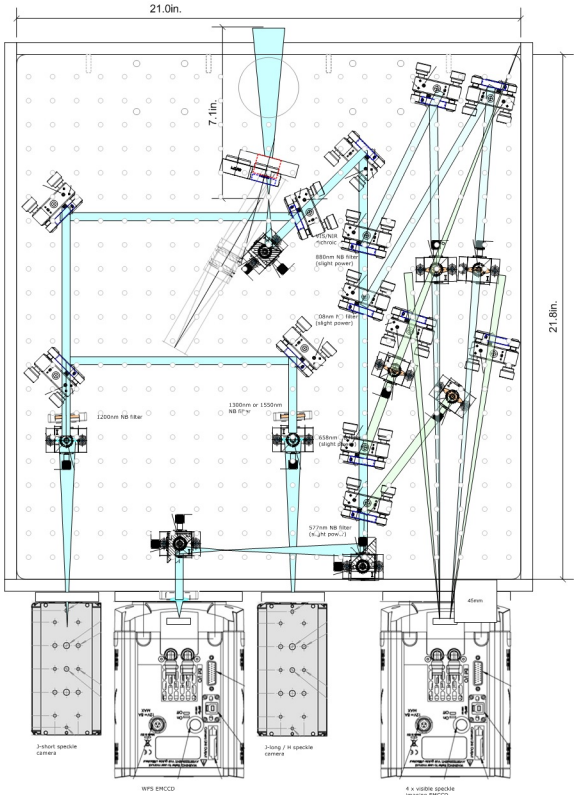

Figure 2: Inside QWSSI, the source beam enters from the top and is split into its visible and NIR components. The NIR side essentially duplicates the current DSSI design. On the visible side, the beam is split off into four optical wavelengths, and the remaining light is sent to the WFS. Not shown here: the acquisition camera and its optics, which are located in the upper left corner of the optics box. The optical design is described in greater detail in Section 2.2.

In addition to the optics for the visible and NIR channels, the optics box includes an in-box, fiber-fed calibration source, as well as an acquisition camera. The acquisition camera is a ZWO ASI178MM with a resolution of 3096$\times$2080, and a pixel size of 2.4μm. All QWSSI's relevant parameters can be found in Table 2.

*Depth of focus scales roughly as f/ratio squared.

Table 2: Relevant parameters.

Parameter	Value	Units
LDT f/ratio	5.97	
PW1000 f/ratio	6.00	
Collimating OAP focal length	50.8	mm
Collimated beam diameter	8.5	mm
Reimaging lenses focal length	400	mm
Andor iXon 888 pixel size	13	μm
Detector size	1024 × 1024	pixels
Sampling rate	25-70	ms per frame
Plate scale (LDT)	8.06	arcsec per mm
	13.3	mas per pix
FOV (LDT)	6.8	arcsec
Diff. limit (LDT)	37.2	mas (HeNe)
Target sensitivity (R-band)	15.5	mag
Plate scale (PW1000)	34.38	arcsec per mm
	56.8	mas per pix
FOV (PW1000)	29.0	arcsec
Diff. limit (PW1000)	159.2	mas (HeNe)
Target sensitivity (R-band)	12.3	mag

The target sensitivity for QWSSI was a R-band magnitude of $R = 15.5$. For the imaging channel, this was largely driven by a couple of rather heuristic considerations. The demonstrated limit of DSSI has been found to be the same value of $R = 15.5$. Given the similarities in the optical channels and detector parameters between DSSI and QWSSI, the design team thought this was reasonable to expect.

For the wavefront channel, a separate (but still rather heuristic) assessment was made. Starting with Mel Dyck's 'Rule of Ten' for wavefront sensors - which is, "a r_0 of 10cm, a t_0 of 10ms, and m_V of 10th mag gives you a SNR of 10" - we set a 7×7 lenslet grid for our Shack-Hartmann WFS. The resultant parameters - a subpupil of 60cm, and a nominal sampling time of 40ms - scale from this rule-of-thumb to indicate a limiting m_V of 15.5. Importantly, this somewhat ad-hoc estimate was consistent with the results from the GWAVES WFS sampling unit that is part of the LDT active optics. In general, our on-sky operational experience has shown that the peak pixel value in the subaperture spots on the WFS EMCCD is roughly twice that of the peak pixel values for the imaging EMCCD.

2.3 Electronics

Relative to its DSSI predecessor, another new QWSSI feature is the QWSSI Timing Generator (QTG). Previous DSSI operations had relied purely on the operator manually initiating a data collection sequence for a given camera from the stock Andor Solis software, and then subsequently starting a second sequence for the second camera manually as well from a second instance of Solis, via point-and-click operations. The resulting twin FITS cubes were typically overlapping in time, but not explicitly synchronized. In order to explicitly synchronize the triggering of all four QWSSI cameras, the QTG was developed, which provides external triggering for the two EMCCDs and the two InGaAs cameras. The module includes a GPS receiver used as a timing reference, and produces sub-millisecond accurate timestamp data for each trigger signal generated during a capture sequence. Each of the four timing channels is independently addressable, resulting in timing sequences from the QTG which can enable, if desired, triggering of certain cameras at multiples of other cameras. For example, one option we will explore in the future is the degree to which the WFS EMCCD should be run at a higher rate than the imager EMCCD.

QWSSI also employs two servo sliders. The first is a linear transition stage that hosts a fold mirror, which can steer the LDT or PW1000 source beam to the acquisition camera. The second is a dual-position slider, which contains a mirror in one position, and is empty in the other. When the empty position is in place, the LDT

source beam is directed through the instrument to the detectors; when the slider is moved to the mirror position, the calibration source is utilized instead.

QWSSI utilizes two on-board Intel Next Unit of Computing (NUC) computers to run the cameras, as well as the electronics (acquisition camera, sliders, calibration source). Since the cameras interface via USB3, no PCI or PCI-e cards are required (as was the case with the previous generation of EMCCDs), allowing the use of these computers. As such, the NUC computers are much smaller than the one used by DSSI, so mounting and dismounting QWSSI from the LDT is much easier, and the weight balance of the instrument is improved. Our original approach was to use a single NUC computer. In principle the USB3 bandwidth is sufficient for handling the data rates from the two EMCCDs and the two InGaAs cameras; however, in practice we found that the USB3 bus of a single NUC computer to be overwhelmed by the data rates. As such, we added a second NUC computer (easily done, given their small size) into the project box, and at present each NUC computer handles a single EMCCD and a single CRED2.

2.4 Mechanical Manufacturing

QWSSI's custom enclosure box and the LDT mounting bracket were manufactured in the Lowell Observatory machine shop out of half-inch plate aluminum. Due to the small overall size (<24"×24"), all parts such as enclosure sidewalls easily fit onto the Haas 5-axis Computer Numerical Control machine in the observatory shop. Plate parts were finished with a black anodization.

In addition to the optics box, QWSSI also includes a Hammond 17"×21.6"×8.1" polycarbonate project box. The project box contains:

- a network-connected power distribution box with webpage-based control of 8 addressable AC power lines
- two EMCCD power supplies and two CRED-2 power supplies
- two Intel NUC computers and their power supplies
- a 16-port USB3 hub and its power supply
- the QTG and its power supply
- the fiber-coupled calibration source, a USB-addressable controller, and the power supply
- a slider power supply

The project box attaches next to QWSSI on the LDT instrument cube on a mounting bracket.

3. OPERATIONS

3.1 Setup

QWSSI was designed to ease the process of mounting and dismounting from both the PW1000 telescope at NPOI (Figure 3) and the LDT (Figure 4). QWSSI boasts a modular design with only two major pieces: the optics box and the project box. Mounting QWSSI can therefore easily be done by two people inside of 90 minutes. The optics box, with the 4 cameras mounted, weighs roughly 125 pounds, and is mounted onto the LDT instrument cube via a hand-operated lift-jack cart. The project box weighs roughly 50 pounds and bolts directly onto an instrument cube strut. USB3 cables, power cables, and trigger cables are then connected from the project box to the cameras, as well as slider power, acquisition camera power and data, and the calibration source fiber optic. From the project box, a single power line, as well as ethernet, connects to ports on the instrument cube.

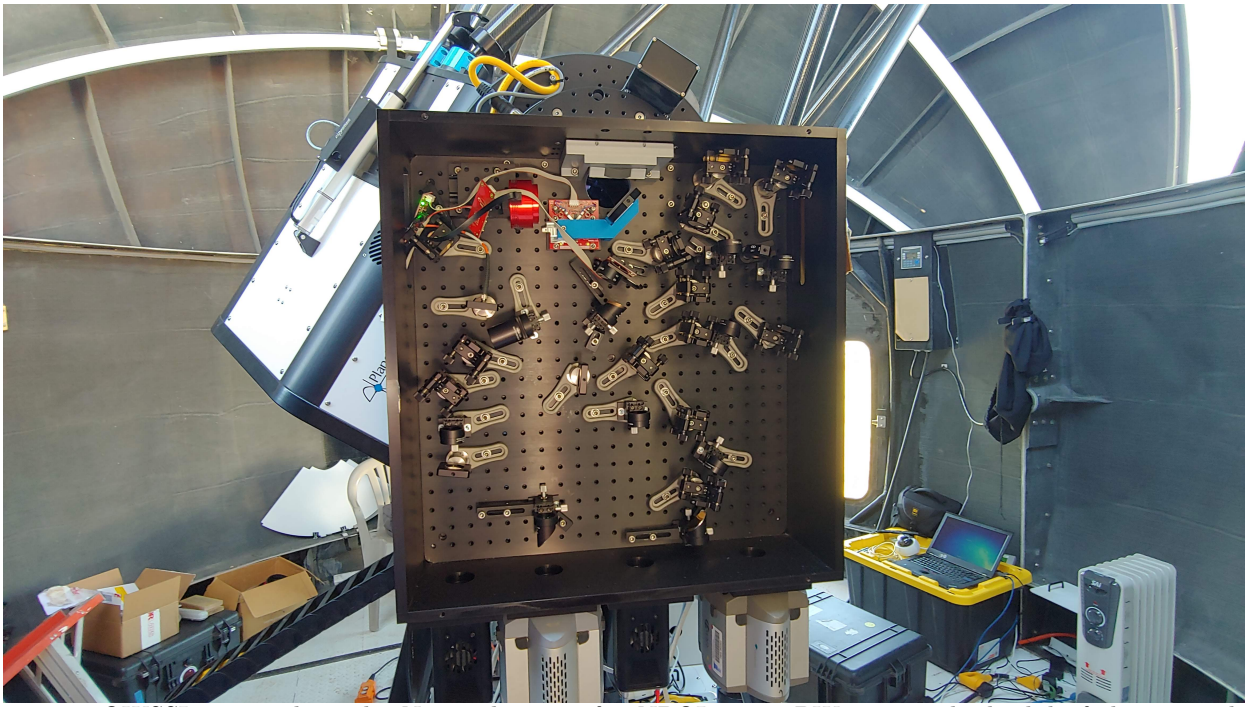

Figure 3: QWSSI mounted on the Nasmyth port of a NPOI 1.0-m PW1000, with the lid of the optics box removed for adjustment of alignments. The instrument's project box rides on the top of the instrument yoke, below the telescope tube swing radius.

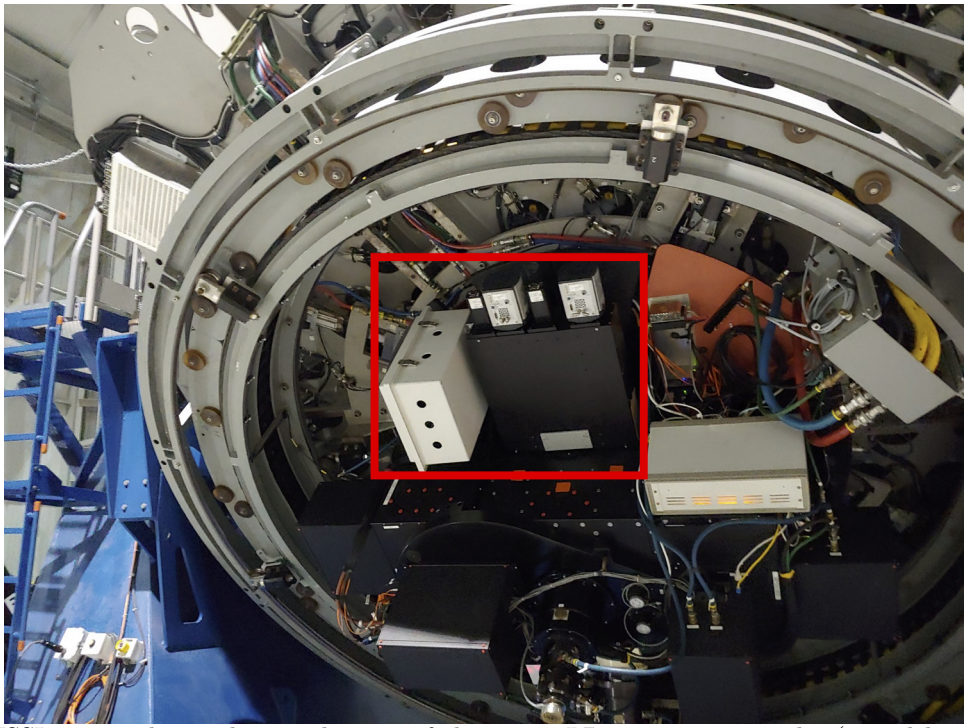

Figure 4: QWSSI mounted on a large side port of the 4.3-m LDT instrument cube (in red box). The design consists of only the optics box (black) and the project box (white), and is therefore easy to maneuver on and off the telescope. QWSSI's small size allows it to fit on any of the LDT ports.

3.2 On-Sky Operations and Data Reduction

During on-sky operations, the observer controls the acquisition camera, sliders, EMCCDs, and InGaAs cameras. We currently utilize stock operations software: ZWO ASIStudio for the acquisition camera, Thorlabs ELLO for the sliders, Andor Solis for the EMCCDs, and First Light Vision for the InGaAs cameras. We access each NUC desktop using either a Remote Desktop Protocol or a Virtual Network Computing client. Previously, with DSSI operations, repetitive operations (such as setting EMCCD gains or exposure times) were automated into single-button actions using AutoHotKey macros, which will similarly develop in the future for more streamlined QWSSI operations.

The files from the EMCCDs and InGaAs cameras are saved as FITS cubes, made up of 1,000 images. These files are then stored on RAID arrays located at Lowell Observatory's Mars Hill campus. As we can generate hundreds of files per night on each of the four cameras, the nightly data volume for a full night of observing is 300-400 gigabytes.

The data reduction pipeline for QWSSI will be able to recover close companions to astronomical objects with magnitude differences of $\Delta m = 5$ for objects inside $\rho = 0.1$ arcseconds. The DSSI pipeline (12), which performs bispectral analysis (13; 14) on each speckle data cube, will form the backbone of the QWSSI pipeline.

4. FUTURE WORK

In the future, we will optimize our operations by implementing changes in several areas. The DSSI code is currently being adapted from IDL to Python and will include several modifications to take full advantage of the QWSSI observations. In particular, the pipeline is being modified to include the Shack-Hartmann WFS data obtained by QWSSI as proposed by Lőbb (2016) (11). This will allow for a better estimation of the PSF in each speckle frame and improve the sensitivity of QWSSI to faint companions by one magnitude over a non-WFS corrected observation. Additionally, we plan to implement wavelength diversity, as QWSSI obtains speckle frames across six different wavelengths ranging from 577 to 1570 nm. With these additions to the data analysis pipeline, we expect the faint companion sensitivity of QWSSI to improve compared to DSSI by 1.5-2.0 magnitudes in the range of 0.1 to 1.0+ arcseconds. Furthermore, we will route a cable from an external antenna to the QTG module to improve GPS signal quality. Ultimately, we should expect timestamps with absolute accuracy of $\pm 50 \mu s$. We will also automate our operations software to optimize the operation of all four cameras at once. Finally, we will replace the Semrock COTS filters with custom, imaging-quality filters to improve the speckle imager beam quality and instrument sensitivity.

QWSSI is already being used in the search for previously undetected M-dwarf companions; however, with the planned optimizations, we will be able to develop tight constraints on characteristics like luminosity and age for these binaries. Furthermore, with QWSSI's NIR channels, we have the potential to create a volume-limited survey of brown dwarf multiplicity. This kind of direct imaging survey would be unprecedented, and would provide insight into the L- and T-dwarfs like never before.

ACKNOWLEDGMENTS

We are grateful to our telescope operators and operations group during commissioning and our first nights of science operations: Amanda Bosh, Victoria Girgis, Ana Hayslip, Ishara Nisley, Sydney Perez, Jason Sanborn, LaLaina Shumar, and Kathryn Turrentine. We thank those in the Lowell Observatory technical group who provided valuable feedback on QWSSI's optical design: Tom Bida, Ted Dunham, Ryan Hamilton, Stephen Levine, Dyer Lytle, and Ralph Nye. We are grateful for the support from Lowell Observatory IT: C. J. von Buchwald-Wright and Scott Do. During our procurement phase, we received extensive support from the Lowell Observatory business office: Lucy Collins, Robin Melena, Le Cam Nguyen, and Diana Weintraub. Finally, we thank Nic Scott for his helpful comments. Support for this project was provided in part by Defense University Research Instrumentation Program awards, as well as NSF Grant No. AST-1616084.

References

[1] Labeyrie, A., "Attainment of Diffraction Limited Resolution in Large Telescopes by Fourier Analysing Speckle Patterns in Star Images," *A&A* **6**, 85 (May 1970).

[2] Horch, E. P., Meyer, R. D., and van Altena, W. F., "Speckle Observations of Binary Stars with the WIYN Telescope. IV. Differential Photometry," *AJ* **127**, 1727–1735 (Mar. 2004).

[3] Tokovinin, A. and Cantarutti, R., "First Speckle Interferometry at SOAR Telescope with Electron-Multiplication CCD," *PASP* **120**, 170 (Feb. 2008).

[4] Horch, E. P., "Speckle imaging at large telescopes: current results and future prospects," in [*Optical and Infrared Interferometry and Imaging V*], Malbet, F., Creech-Eakman, M. J., and Tuthill, P. G., eds., *Society of Photo-Optical Instrumentation Engineers (SPIE) Conference Series* **9907**, 99070J (Aug. 2016).

[5] Horch, E. P., Veillette, D. R., Baena Gallé, R., Shah, S. C., O'Rielly, G. V., and van Altena, W. F., "Observations of Binary Stars with the Differential Speckle Survey Instrument. I. Instrument Description and First Results," *AJ* **137**, 5057–5067 (June 2009).

[6] Horch, E. P., Gomez, S. C., Sherry, W. H., Howell, S. B., Ciardi, D. R., Anderson, L. M., and van Altena, W. F., "Observations of Binary Stars with the Differential Speckle Survey Instrument. II. Hipparcos Stars Observed in 2010 January and June," *AJ* **141**, 45 (Feb. 2011).

[7] Scott, N. J., Howell, S. B., Horch, E. P., and Everett, M. E., "The NN-explore Exoplanet Stellar Speckle Imager: Instrument Description and Preliminary Results," *PASP* **130**, 054502 (May 2018).

[8] Scott, N. J. and Howell, S. B., "NESSI and 'Alopeke: two new dual-channel speckle imaging instruments," in [*Optical and Infrared Interferometry and Imaging VI*], Creech-Eakman, M. J., Tuthill, P. G., and Mérand, A., eds., *Society of Photo-Optical Instrumentation Engineers (SPIE) Conference Series* **10701**, 107010G (July 2018).

[9] Scott, N. J., "'Alopeke, Zorro, and NESSI: Three dual-channel speckle imaging instruments at Gemini-North, Gemini-South, and the WIYN telescopes.," in [*AAS/Division for Extreme Solar Systems Abstracts*], *AAS/Division for Extreme Solar Systems Abstracts* **51**, 330.15 (Aug. 2019).

[10] Calef, B., "Improving imaging through turbulence via aperture partitioning," in [*Visual Information Processing XIX*], Rahman, Z.-U., Reichenbach, S. E., and Neifeld, M. A., eds., *Society of Photo-Optical Instrumentation Engineers (SPIE) Conference Series* **7701**, 77010G (Apr. 2010).

[11] Lőbb, J., *Speckle Image Enhancement Using Recorded Shack- Hartmann Wavefront Sensor Data*, Master's thesis, Southern Connecticut State University, New Haven, Connecticut (Apr. 2016).

[12] Horch, E. P., van Altena, W. F., Cyr, William M., J., Kinsman-Smith, L., Srivastava, A., and Zhou, J., "Charge-Coupled Device Speckle Observations of Binary Stars with the WIYN Telescope. V. Measures During 2001-2006," *AJ* **136**, 312–322 (July 2008).

[13] Lohmann, A. W., Weigelt, G., and Wirnitzer, B., "Speckle masking in astronomy: triple correlation theory and applications.," *Appl. Opt.* **22**, 4028–4037 (Dec. 1983).

[14] Meng, J., Aitken, G. J. M., Hege, E. K., and Morgan, J. S., "Triple-correlation subplane reconstruction of photon-address stellar images.," *Journal of the Optical Society of America A* **7**, 1243–1250 (July 1990).